2018 European Control Conference (ECC)
June 12-15, 2018. Limassol, Cyprus

Efficient Multi-Objective and Multi-Scenarios Control Synthesis Methodology for Designing a Car Lane Centering Assistance System

Simon Mustaki[1,2], Philippe Chevrel[1], Mohamed Yagoubi[1] and François Fauvel[2]

Abstract— **This paper presents a methodology to design an optimized Lane Centering assistance (LCA) system for an imposed structure. It proceeds within the H_2/H_∞ framework to manage the trade-off between lane centering and comfort. At a first stage, convenient indicators are defined in a way to be understandable, closely linked to practical specifications, and easy to compute. Some of them require using exogenous signal model (e.g. curves or gusts of wind), giving *a priori* information on possible scenarios. Based on them, a multi-scenarios and multimodel robust control problem is built, closely linked to the initial requirements. It aims to minimize the jerks of the lateral error and the steering wheel induced by the disturbances, under constraints of performance and robustness specifications. Deterministic non-smooth optimization algorithms are considered to solve it. The efficiency and the robustness of the synthesized controller is demonstrated by simulation using real measurements of a camera. Lastly, the proposed methodology makes future adaptation to other ADAS easier, which is a crucial point in an industrial context.**

I. INTRODUCTION

A fully autonomous vehicle is widely considered to be the best way to reduce the road accidents. With this aim, numerous Advanced Driving Assistance Systems (ADAS) have been introduced in new vehicles in order to improve safety, comfort and consumption. This work focuses on lateral control and more precisely on Lane Centering Assistance (LCA) which seeks to center the vehicle in the lane. Although researchers and engineers have been working on the design and control of the LCA system over the past two decades, it has only recently been introduced in large-scale vehicles and therefore legislation still limits its use by requiring the driver to be in charge (SAE level 1 or 2 of autonomy [1]). This means that drivers must keep their hands on the steering wheel all the time and the assistance should work correctly despite the induced torque disturbance, while giving a comfortable steering wheel feeling and allow take over if needed. The performance and stability of lateral control depend significantly on the steering system characteristics, the tire-road contact and the quality of the sensors. Car manufacturers have therefore implemented a driving assistance system that either deals with lateral control in autonomy (the action of the driver on the steering wheel is seen as a disturbance) or supplements the driver's action (known as *shared steering control* [2] [3]). These lateral control strategies are traditionally based on the well-known bicycle model and are associated with the equations given by e.g. [4] or [5] (and references therein).

Usefulness and user-friendliness are the key factors of the acceptability of lateral assistance by the general public. Therefore, engineers must include in their tuning process some criteria that take into account safety, performance and comfort. For example, an efficient assistance should minimize the lateral error as well as the driver's interventions, while a safe one would favor the respect of the states' amplitude and speed variation limitations (to ensure safety and the possibility of take over by the driver).

Motivated by the craze for the ADAS systems, academic as well as industrial researchers have explored a broad spectrum of techniques to synthesize controllers [4] [6]. Among recent papers, the Model Predictive Control (MPC) technique is widely used for the lateral control problem. For example, performance and safety guarantees are derived in [7] in which the controller's stability is assessed through the invariant set theory. As almost every vehicle's characteristics depend on longitudinal speed, the Linear Parameter Varying (LPV) control approach has turned out to be very useful. In [8], the authors use an LPV control approach to deal with the nonlinear characteristics of the tires whereas a robust LPV H_2 static output feedback controller is synthesized in [9]. In the latter, the physical limitations of the vehicle's longitudinal acceleration are considered in order to reduce the conservatism and the whole controller is derived from Linear Matrix Inequality (LMI) specifications. An other technique to manage a time-varying system is to define the whole model as a set of sub-models with switching rules, as carried out in [10] in which a switched H_∞ controller is proposed. The difficulty of such a methodology lies in handling the stability analysis, which is carried out through LMI constraints. An H_2-preview control is applied in [11]. Similarly to the MPC technique, it includes knowledge of the path to follow in the future (with a finite horizon) and can also deal with the delays in the loop.

This paper investigates a multi-objective control strategy to optimize a LCA system whose structure and parameterization are specific and constrained. It aims to formalize soft and hard constraints as close as possible to realistic specifications in terms of performance and robustness (the *soft constraints* designate the cost function which will be minimized whereas the *hard constraints* designate those which must be

[1]IMT Atlantique, LS2N Laboratory, UBL, 44307 Nantes, France {simon.mustaki,philippe.chevrel,mohamed.yagoubi}@ls2n.fr

[2]Renault S.A.S., 1 avenue du Golf, 78280 Guyancourt, France {simon.mustaki,françois.fauvel}@renault.com

satisfied). The methodology uses non-smooth optimization techniques in a H_2/H_∞ control framework (including environment/scenarios modeling). The criteria together with the scenarios considered here have been carefully chosen to have a comprehensive impact on the vehicle's behavior.

This paper is organized as follows. In Section II, after introducing the state-space model associated with the whole controller architecture, the methodology to synthesize an efficient LCA controller is discussed. The simulation results, in which real measured data are used as the input, are given in Section III. Lastly, concluding remarks and future directions are provided in Section IV.

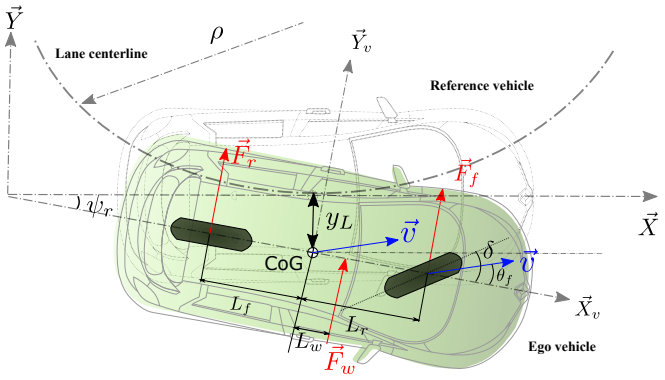

Fig. 1. Notations of the bicycle model

II. Control Strategy

A. Linear Vehicle Model

The model used in this paper is the well-known linear bicycle model, represented in Figure 1. Normal driving situations are considered and therefore the assumptions made to derive this model are: (i) the longitudinal speed is constant, (ii) the considered angles stay small enough, (iii) the lateral tire forces are proportional to the slip angle. We denote $\theta_{f,r}$, $C_{f,r}$, $F_{f,r}$ and $L_{f,r}$ as the cornering angles, cornering stiffness, tire forces and distance from center of gravity to axles, for front and rear wheels, respectively. Moreover, $\dot{\psi}$ is the yaw rate, ψ_r the relative yaw angle which designates the difference between the vehicle yaw angle ψ and the ideal yaw angle $\psi_i = v_x\rho$ defined by the lane centerline [12] ; y_L is the lateral error ; v_x and $v_y = \dot{y}_L$ are the longitudinal and lateral speed, respectively. Two disturbances are taken into account : the curvature of the road ρ and the wind force F_w.

TABLE I
Vehicle Model Parameters

Parameter	Description	Value	Uncertainty
C_f	Front cornering stiffness	123170 N/rad	±10%
C_r	Rear cornering stiffness	139600 N/rad	±10%
M	Total mass of the vehicle	1900 kg	[1800 2400]
I_z	Vehicle yaw moment of inertia	3846 kg.m^2	[3700 3900]
L_{tot}	Wheelbase of the vehicle	2.884 m	-
L_f	Distance between CoG and front axle	1.117 m	±10%
L_r	Distance between CoG and rear axle	$L_{tot} - L_f$	[1.6553 1.8787]
L_w	Distance between CoG and point of application of wind force	0.1 m	-
n_s	Steering gear ratio	16.34	-
ξ_s	Steering system damping	$\sqrt{2}/2$	-
ω_s	Steering pulsation	18.85 rad/s	-
v_x	Vehicle longitudinal speed	90 km/h	-

The Electric Power Steering (EPS) is defined as a 2$^{\text{nd}}$ order system whose parameters are the natural frequency ω_s, the damping ratio ξ_s and the ratio n_s between the front wheel angle δ and the steering wheel angle δ_{sw}:

$$\frac{\delta}{\delta_{sw}} = \frac{n_s\omega_s^2}{s^2 + 2\xi_s\omega_s s + \omega_s^2} \tag{1}$$

B. Control-Based State Model

The complete road-vehicle model can be written as follow:

$$\dot{x} = Ax + B_u u + B_w w \tag{2}$$

where $x = [\dot{\psi} \;\; \psi_r \;\; \dot{y}_L \;\; y_L \;\; \dot{\delta} \;\; \delta \;\; -\int y_L]^T$ is the vehicle state space vector (augmented by the integral of the lateral error), $w = [\rho \;\; F_w]^T$ is the disturbance vector and u is the control input corresponding to the steering wheel angle. The system matrices of (2) are given as follows:

$$A = \begin{bmatrix} a_{11} & a_{12} & a_{13} & 0 & 0 & a_{16} & 0 \\ 1 & 0 & 0 & 0 & 0 & 0 & 0 \\ a_{31} & a_{32} & a_{33} & 0 & 0 & a_{36} & 0 \\ 0 & 0 & 1 & 0 & 0 & 0 & 0 \\ 0 & 0 & 0 & 0 & a_{55} & a_{56} & 0 \\ 0 & 0 & 0 & 0 & 1 & 0 & 0 \\ 0 & 0 & 0 & -1 & 0 & 0 & 0 \end{bmatrix}, \quad B_u = \begin{bmatrix} 0 \\ 0 \\ 0 \\ 0 \\ n_s\omega_s^2 \\ 0 \\ 0 \end{bmatrix},$$

$$B_w = \begin{bmatrix} 0 & -v_x & -v_x^2 & 0 & 0 & 0 & 0 \\ \frac{L_w}{I_z} & 0 & \frac{1}{M} & 0 & 0 & 0 & 0 \end{bmatrix}^T$$

with

$$a_{11} = \frac{-(C_f L_f^2 + C_r L_r^2)}{I_z v_x}, \quad a_{12} = \frac{C_f L_f - C_r L_r}{I_z}, \quad a_{13} = \frac{-(C_f L_f - C_r L_r)}{I_z v_x},$$
$$a_{16} = \frac{C_f L_f}{I_z}, \quad a_{31} = \frac{-(C_f L_f - C_r L_r)}{M v_x}, \quad a_{32} = \frac{C_f + C_r}{M},$$
$$a_{33} = \frac{-(C_f + C_r)}{M v_x}, \quad a_{36} = \frac{C_f}{M}, \quad a_{55} = -2\xi_s\omega_s, \quad a_{56} = -\omega_s^2,$$

It is considered that the only unmeasurable states are $\dot{y}_L$ and $\dot{\delta}$. Hence, the output equation of the system (2) is given by $y = Cx$ with

$$C = \begin{bmatrix} 1 & 0 & 0 & 0 & 0 & 0 & 0 \\ 0 & 1 & 0 & 0 & 0 & 0 & 0 \\ 0 & 0 & 0 & 1 & 0 & 0 & 0 \\ 0 & 0 & 0 & 0 & 0 & 1 & 0 \\ 0 & 0 & 0 & 0 & 0 & 0 & 1 \end{bmatrix}$$

Figure 2 presents the system structure. An observer is implemented in the control loop to reconstruct the two unmeasurable states. Here, the observer is imposed and cannot be modified. In addition, a feedforward is used to anticipate the effect of the curvature. To this end, the feedforward will add an extra steering wheel angle to the one calculated by the feedback part, and correct the output vector to remove part of the effect of the curvature on the states. This correction is based on a static inversion of the model, that is leading to $\dot{X} = 0$ for a given curvature ρ and a longitudinal speed v_x. Lastly, K is a state-feedback controller using the estimated state $\hat{x}$.

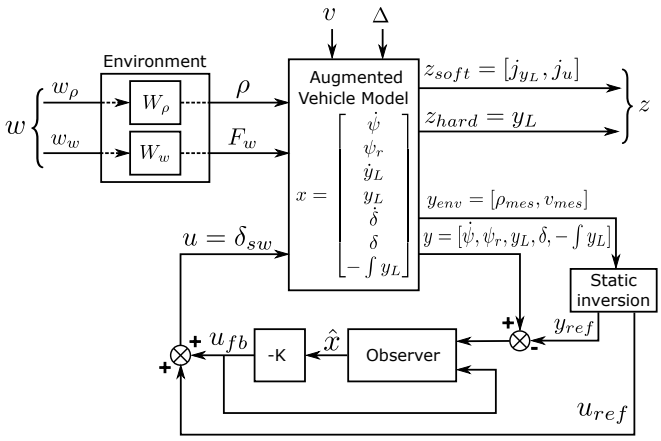

Fig. 2. Conceptual schema for synthesis

C. Control Problem Formulation

The assistance to be synthesized should improve the safety and comfort of the passengers in normal driving situations, guaranteeing to be effective despite the unavoidable variations in the vehicle's parameters and the variability of the environment. Our proposition is thus to carry out the synthesis of the structured controller in a multi-objective and multi-scenarios setting, and for a set of uncertain linear bicycle models. Remembering that the state feedback gains inside matrix K are the only free parameters, the aim in this paper is the direct optimization of the robustness properties and the performance of the whole closed-loop, without modifying the structure that is imposed here. The challenge is twofold: first, to formalize an *ad hoc* multi-objective and multi-scenarios optimization problem; second to find K solving this problem. For the formalization of the optimization problem, a methodology is proposed that includes a choice of pertinent signals for performance analysis, input signals and scenario modeling based on real dynamic characteristics and finally a multi-model approach to apprehend the parametric robustness. The main idea here is to minimize the jerks of the lateral error and of the steering wheel angle caused, for instance, by the road curvature or the wind.

In order to provide some information about the disturbance dynamics, generator models are considered, which may be seen as input shaping filters. The controller will use this information to predict and anticipate the system evolution, which will improve its overall behavior [13]. Hence, defining such generator models constitutes the particular way proposed here to specify and formalize the environment of the system. Their inputs are irreducible signals such as impulse or white noise (e.g. random pulse train), and their outputs define the particular disturbance considered (see e.g. Figure 3). The output $\mathscr{L}_2$-norm from the irreducible signals to the controlled output of the system is directly linked to the H_2 norm of the corresponding transfer (see Appendix B). We will use this property hereafter to define an *ad hoc* multi-objective and multi-criteria control problem.

Road Curvature Model: The dynamics of the road curvature are dependent on the maximum permitted speed. For example, according to [14], for a 90 km/h limited road without road banks, the maximum radius of the road should be 318 meters, i.e. $\rho_{max} = \frac{1}{318} = 0.0031\ m^{-1}$. Moreover, a turn settles in a few seconds so the time constants can be chosen appropriately. A 3rd order Markov model is consequently chosen to take into account the strong continuity of the road curvature plus a null derivative at the initial time:

$$\frac{\rho}{w_\rho} = \frac{K}{(1+\tau s)(\frac{s^2}{\omega_0^2} + \frac{2\xi}{\omega_0}s + 1)} = W_\rho$$

Wind Model: The wind model is here a 2nd order:

$$\frac{F_w}{w_w} = \frac{K}{\frac{s^2}{\omega_0^2} + \frac{2\xi}{\omega_0}s + 1} = W_w$$

The impulse responses of the two proposed predictive models are shown in Figure 3.

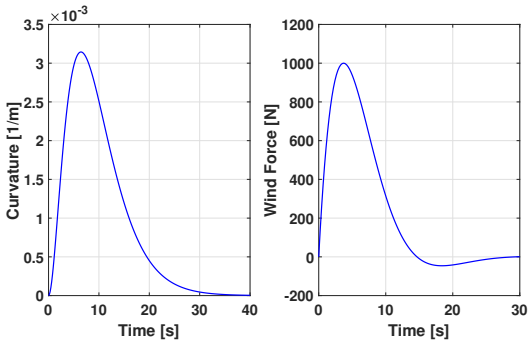

Fig. 3. Impulse responses of the road curvature (for 90 km/h) and of the wind models

Finally, the control problem is written as follows (see Figure 2):

$$
\begin{aligned}
\underset{x\in\mathscr{X}}{\text{minimize}} \quad & \|T_{w_w\to j_u}\|_2, \|T_{w_w\to j_{y_L}}\|_2, \|T_{w_\rho\to j_u}\|_2, \|T_{w_\rho\to j_{y_L}}\|_2 \\
\text{subject to} \quad & \|T_{w_w\to y_L}\|_2 < k_w \\
& \|T_{w_\rho\to y_L}\|_2 < k_\rho \\
& M_{dyn} = \|sT_u(s)\|_\infty^{-1} > \tau_{min} \\
& Mm_u = \|S_u(s)\|_\infty^{-1} > 0.5
\end{aligned}
$$

where

- j_u and j_{y_L} are the jerk signals of the steering wheel angle and the lateral error, respectively.
- k_w and k_ρ are constant values specified by the user, which lets him/her choose the trade-off between performance and minimization of the objective.
- $S_u(s)$ and $T_u(s)$ are the sensitivity and the complementary sensitivity functions, respectively, at the input.
- M_{dyn} is the dynamic margin (or the generalized delay margin, cf. Appendix A) at the input and τ_{min} its minimum expected value.
- Mm_u is the input multivariable module margin.
- $\mathscr{X}$ is the domain of research.

The multi-objective control problem presented above does not have any analytical solution. Besides, it is neither a convex nor a smooth optimization problem. To address such an optimization problem, the authors chose to use recently developed non-smooth optimization algorithms, which offer significant advantages. They are natively able to cope with a structured controller (PID, observer state-feedback, general static output feedback), in a multi-objective and multi-criteria (H_2, H_∞) framework. They do this within a reasonable computational time due to the use of (sub)gradients and the fact that they optimize the parameters directly instead of searching for full-order Lyapunov matrices (as is the case with LMI approaches). Currently, at least two different Matlab toolboxes are based on non-smooth optimization: the *systune* solver [15] [16] and the *HIFOO* one [17] [18]. A comparison between these two tools is given in [16]. In this work, the *systune* function of Matlab's Control System Toolbox was chosen over HIFOO due to its deterministic algorithm and its ability to treat such a control problem well.

The minimization of the jerks should give a smooth behavior of the lateral control, comfortable for the passengers, and saturation of the actuator should be avoided. The first two hard constraints are the performance constraints and express the fact that the energy of the lateral error signal should be "small", despite the potential disturbances. The parameters k_ρ and k_w manage the compromise between the performance of the system and its acceptability by the driver. In fact, increasing these parameters will relax the constraints on the lateral error and hence enable smoother responses of the jerks, leading to a better acceptability by drivers. The third hard constraint $M_{dyn} > \tau_{min}$ is to constrain the robustness against uncertainty such as time delay (cf. Appendix A) or neglected dynamics. Finally, the last hard constraint $Mm_u > 0.5$, thanks to the circle criterion (see ref [19]) ensures the robustness of the closed-loop in spite of the uncertain behavior of the electric power steering system (EPS).

Moreover, by specifying that some parameters are uncertain (see Table I), a controller that robustly meets performance goals over multiple plant configurations may be obtained by multi-model synthesis. The software works in two steps: first, it searches for the set in which the hard constraints are respected despite the uncertainties; secondly, it minimizes the cost function over this set. It returns the nominal and the worst case values of the soft and hard constraints, which is an indicator of how robust the controller will be. Lastly, the optimization algorithms implemented in *systune* perform local optimization. The solution then potentially depends on the initialization stage. However, we noticed that a basic random initialization very often converges towards the same solution. To validate our controller, a lateral error of less than 20 *cm* is expected in the soft curves with a maximal error of 30 *cm* in the tight curves, the distance from which the driver is disturbed and may take over the assistance. A smooth steering wheel angle is also aimed for to meet safety requirements. In addition, the lateral acceleration should be less than 2 $m.s^{-2}$ for the comfort of the passengers.

III. SIMULATION RESULTS

In this section, some simulation results are provided based on real track measurements. Hence, the measured curvature and speed of a real test on a track are the inputs of the simulation. The control problem presented above is carried out for several reference longitudinal speeds: 55 km/h, 70 km/h and 90 km/h. Then, a function is implemented in the simulation to interpolate linearly the state feedback gains in real-time between each reference speed (piecewise linear interpolation over the whole speed range).
For each of these speeds, the predictive model's amplitude for the road curvature used in the synthesis is adapted and the value of the hard constraints are: $\tau_{min} = 0.2$ *s*, $k_w = k_\rho = 0.5$. The test track is presented in Figure 4 and the measurements of the curvature associated with the speed profile (almost constant speed) are shown in Figure 5.

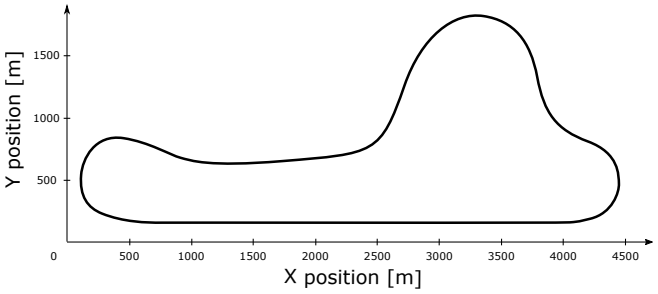

Fig. 4. Test track

Figure 6 associated with Figure 7 shows the robustness of the design methodology proposed with 10 random sets

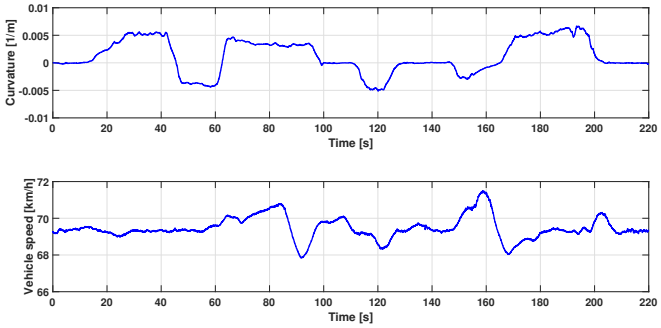

Fig. 5. Curvature and Speed profiles

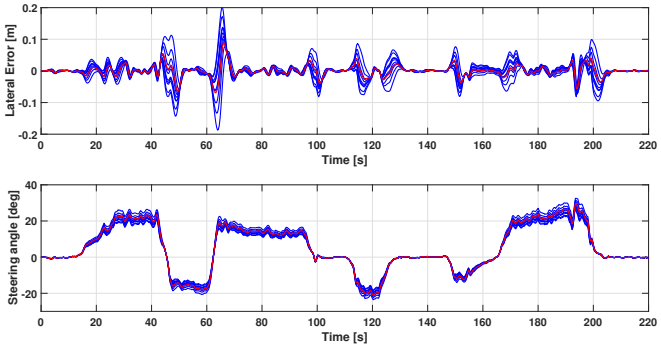

Fig. 6. Lateral error (top) and steering angle (bottom) simulation responses of 10 random sets of uncertain parameters (blue) and of the nominal one (red)

of parameters (in blue) compared to the nominal values of the parameters (in red). First, it is noticeable that the lateral error is always less than 20 *cm*, which is a remarkable performance, even if the curves are rather tight (relative to 70 km/h) and secondly the range of the responses is very narrow, which proves the robustness of the control law. The measurements of the curvature are a bit noisy, which can be seen in the steering angle and lateral error responses, but *a priori* these responses will be less sensitive to the noise in a real car because of the natural damping of the car and its EPS, which is not modeled entirely here.

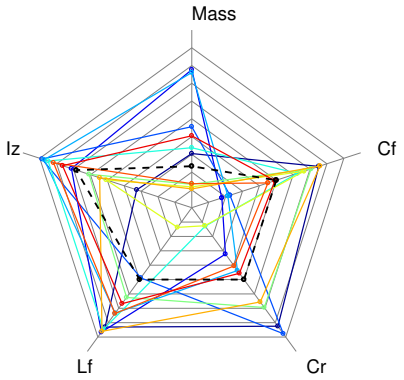

Fig. 7. Dispersion of uncertain parameters for the simulations above. The black dashed line represents the nominal values. The center of the spiderweb corresponds to the minimum values of the parameters and the exterior to the maximum ones

Figure 8 shows the impact of the parameter k_ρ on the vehicle's behavior. The command is less reactive when k_ρ increases, which leads to a smoother response of the steering wheel (and thus a smoother behavior of the vehicle and a better acceptability by the user) but at the cost of a poorer performance. This is because the command filters the noise of the measured curvature better as k_ρ increases. These parameters are essential in the trade-off between performance and acceptability.

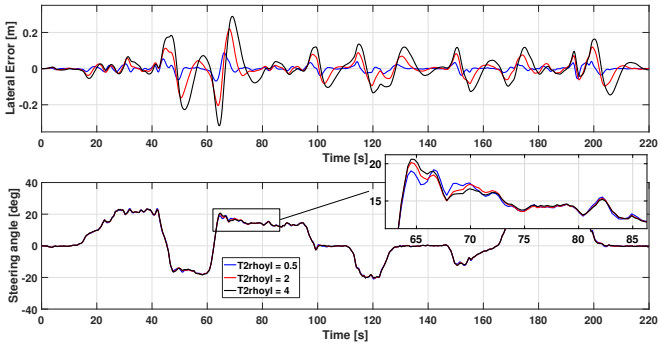

Fig. 8. Variation of the parameter k_ρ

IV. CONCLUSIONS

This paper proposes a methodology to design an optimized Lane Centering Assistance system. It proceeds in the H_2/H_∞ framework, by carefully defining convenient indicators, which are understandable, closely linked to practical specifications, and easy to compute. What we call a multi-scenario approach is used to consider performance with regard to different cases of use, e.g. curves or gusts of wind. It proceeds by modeling potential and realistic exogenous signals such as curvature and wind. Then, the $\mathscr{L}_2$-norm of some chosen output signals (e.g. lateral error, jerks) may be evaluated through H_2 or H_∞ norms. Moreover, static and dynamic margins are used and evaluated as H_∞ norms of specific transfers to assess robustness. Finally, parametric uncertainties are explicitly taken into account by using multi-model synthesis. The multi-scenario and multi-objective methodology proposed is consistent, and leads to an optimized solution, whose structure was *a priori* set according to engineering considerations. Technically, the optimization problem considered is non-convex and non-smooth. For computational speed considerations, we prefer to use subgradients with the risk of obtaining a local solution, rather than global optimization tools or proceeding to convex relaxation. A careful initialization prevents from the risk of a poor local optimum.

The solution obtained is reproducible and simulation leads to very encouraging results. Hence, implementation in a real vehicle is planned. A good performance is expected, even with the difference between modeling and reality, due to the dynamic margin, which ensures robustness against neglected dynamics (and particularly at high frequencies). Future works will focus on the proof of stability of the controller at all

speeds, considering limitations in the variation of longitudinal acceleration as well as on integrating the sensor's model with noise.

APPENDIX

A. Dynamic Margin or the Generalized Delay Margin [20] [21]

Let us consider a process $G(s)$, a stabilizing regulator $K(s)$ and the associated open-loop transfer $L(s) = G(s)K(s)$, strictly proper. $T = L/(L+1)$ denotes the complementary sensitivity function. The dynamic margin is defined as follows:

$$M_{dyn} = \inf_{\omega} \frac{1}{|\omega T(j\omega)|} = \frac{1}{\sup_{\omega} |\omega T(j\omega)|} = \|sT(s)\|_{\infty}^{-1} \quad (3)$$

and it is homogeneous to a time. We will demonstrate that $M_{dyn} < M_d$, where $M_d = M_\Phi/\omega_c$ is the delay margin, M_Φ the phase margin and ω_c the critical frequency for which we have $|L(j\omega_c)| = 1$. By definition,

$$|T(j\omega_c)| = \frac{|L(j\omega_c)|}{|1+L(j\omega_c)|} = \frac{1}{|1+L(j\omega_c)|} \quad (4)$$

With the diagram in Figure A.1 (the blue segment is smaller than the red arc), we can assert that:

$$\underbrace{|1+L(j\omega_c)|}_{1/|T(j\omega_c)|} < M_\Phi = \omega_c M_d \quad (5)$$

Hence, by combining equations (4) and (5), we obtain:

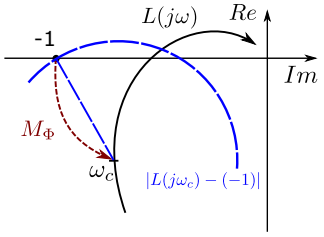

Fig. A.1. Nyquist plot and margins

$$\frac{1}{|T(j\omega_c)|} < \omega_c M_d \Rightarrow \frac{1}{|\omega_c T(j\omega_c)|} < M_d$$
$$\Rightarrow \inf_{\omega} \frac{1}{|\omega T(j\omega)|} < M_d$$
$$\Rightarrow M_{dyn} < M_d$$

B. Input-Output Relationships [22, Chap 4, p 105]

Table II shows the relationships between a Dirac input and the output norms. This highlights the interest of using Dirac inputs (w_w and w_ρ) for modeling the disturbances (F_w and ρ): on the one hand, minimizing the H_2-norm of G reduces indeed the $\mathscr{L}_2$-norm of y, i.e. the impact of the signal u on the output signal y. On the other hand, deriving predictive models from such input and through an impulse response ensures that the resulting signal never exceeds the greatest value attained by this impulse response. For example, the gain K of W_ρ is adjusted in order to match the maximum road curvature ρ_{max}.

TABLE II

OUTPUT NORMS FOR A DIRAC INPUT $\delta(t)$ OR A WHITE NOISE $w(t)$. g DESIGNATES THE IMPULSE RESPONSE FROM u TO y AND G THE LAPLACE TRANSFORM OF g

	$\mathbf{u(t)} = \delta(\mathbf{t})$ or $\mathbf{w(t)}$
$\|\mathbf{y}\|_2$	$\|G\|_2$
$\|\mathbf{y}\|_\infty$	$\|g\|_\infty$

REFERENCES

[1] SAE International, "Levels of driving automation," https://www.sae.org/misc/pdfs/automated_driving.pdf, 2016.

[2] L. Saleh, P. Chevrel, F. Claveau, J.-F. Lafay, and F. Mars, "Shared steering control between a driver and an automation: Stability in the presence of driver behavior uncertainty," *IEEE Transactions on Intelligent Transportation Systems*, vol. 14, no. 2, pp. 974–983, 2013.

[3] A.-T. Nguyen, C. Sentouh, and J.-C. Popieul, "Driver-automation cooperative approach for shared steering control under multiple system constraints: Design and experiments," *IEEE Transactions on Industrial Electronics*, vol. 64, no. 5, pp. 3819–3830, 2017.

[4] R. Rajamani, *Vehicle dynamics and control*. Springer Science & Business Media, 2011.

[5] H. Pacejka, *Tire and vehicle dynamics*. Elsevier, 2005.

[6] A. Eskandarian, *Handbook of intelligent vehicles*. Springer, 2012.

[7] L. Ni, A. Gupta, P. Falcone, and L. Johannesson, "Vehicle lateral motion control with performance and safety guarantees," *IFAC-PapersOnLine*, vol. 49, no. 11, pp. 285–290, 2016.

[8] B. Németh, P. Gáspár, and J. Bokor, "LPV-based integrated vehicle control design considering the nonlinear characteristics of the tire," in *American Control Conference (ACC), 2016*. American Automatic Control Council (AACC), 2016, pp. 6893–6898.

[9] A.-T. Nguyen, P. Chevrel, and F. Claveau, "On the effective use of vehicle sensors for automatic lane keeping via lpv static output feedback control," in *IFAC World Congress*, 2017.

[10] L. Menhour, D. Koenig, and B. D'Andréa-Novel, "Simple discrete-time switched H_∞ optimal control: Application for lateral vehicle control," *IFAC-PapersOnLine*, vol. 48, no. 26, pp. 43–48, 2015.

[11] L. Saleh, P. Chevrel, and J.-F. Lafay, "Generalized H_2-preview control and its application to car lateral steering," *IFAC Proceedings Volumes*, vol. 43, no. 2, pp. 132–137, 2010.

[12] H. Peng and M. Tomizuka, "Lateral control of front-wheel-steering rubber-tire vehicles," *California Partners for Advanced Transit and Highways (PATH)*, 1990.

[13] P. Chevrel, *Methodology of the State Approach Control*. Philippe de Larminat, *Analysis and Control of Linear Systems*, 2013, Wiley-ISTE, pp.55, Wiley-ISTE, 978-1-118-61385-6.

[14] Sétra, "Comprendre les principaux paramètres de conception géométrique des routes, p15," http://www.infra-transports-materiaux.cerema.fr/IMG/pdf/conception_geometrique_route.pdf, 2006.

[15] P. Apkarian, P. Gahinet, and C. Buhr, "Multi-model, multi-objective tuning of fixed-structure controllers," in *2014 European Control Conference (ECC)*. IEEE Publ. Piscataway, NJ, 2014, pp. 856–861.

[16] P. Apkarian and D. Noll, "Optimization-based control design techniques and tools," *Encyclopedia of Systems and Control*, 2015.

[17] J. Burke, D. Henrion, A. Lewis, and M. Overton, "HIFOO - a Matlab package for fixed-order controller design and H_∞ optimization," in *Fifth IFAC Symposium on Robust Control Design, Toulouse*, 2006.

[18] S. Gumussoy, D. Henrion, M. Millstone, and M. L. Overton, "Multi-objective robust control with HIFOO 2.0," *IFAC Proceedings Volumes*, vol. 42, no. 6, pp. 144–149, 2009.

[19] M. Safonov and M. Athans, "A multiloop generalization of the circle criterion for stability margin analysis," *IEEE Transactions on Automatic Control*, vol. 26, no. 2, pp. 415–422, 1981.

[20] P. de Larminat, *Automatique appliquée*. Hermès Science: Lavoisier, 2007.

[21] Y.-P. Huang and K. Zhou, "Robust stability of uncertain time-delay systems," *IEEE Transactions on Automatic Control*, vol. 45, no. 11, pp. 2169–2173, 2000.

[22] K. Zhou, J. C. Doyle, K. Glover *et al.*, *Robust and optimal control*. Prentice hall New Jersey, 1996, vol. 40.